CHAPTER 3

FAR-INFRARED AND RAMAN SPECTRA OF THE SOLID PHASES OF CBOOA

3.1. Introduction

The vibrational spectra of liquid crystalline materials have been useful in elucidating the structure of the different phases exhibited by them. Previous studies have shown that the spectra observed in the various phases can yield significant information regarding the nature of the order and intermolecular forces,[1-4] molecular conformations[5-6] as well as certain characteristics of the phase transitions.[7-9] While most of the studies so far have dealt with nematogenic materials, relatively fewer studies are available on the vibrational spectra of liquid crystals exhibiting the smectic phase as well.[10,11] Smectogenic materials are of particular interest in the light of current theories which indicate the possibility of a second order phase change in the case of smectic C-smectic A I and smectic A-nematic[13-15] transitions. In this connection, CBOOA (N-p-cyanobenzilidene-p-n-octyloxy aniline) whose molecular formula is shown in Fig. 3.1, has attracted considerable attention recently because it undergoes the smectic A-nematic transition. Several experimental studies have been carried out to determine

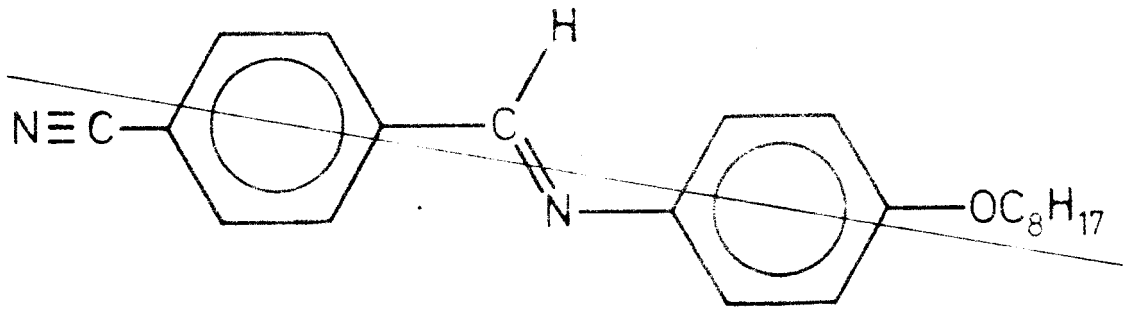

FIGURE 3.1

Molecular structure of CBOOA. The long axis of the molecule is taken to be the line joining the centres of the two benzene rings.

the variation of its specific heat[16] (C_p), magnetic susceptibility,[16] light scattering[17] as wall as elastic constants[18,19] *in* the vicinity of this transition, in order to ascertain the order of the transition. Thus, CBOOA offers an interesting case for the study of vibrational spectra in its different phases and such information should prove helpful in correlating their structural characteristics.

With this aim, we have undertaken a spectroscopic study of CBOOA. The results *of* our study on liquid crystalline CBOOA are presented in the next chapter* Here we present the results of a far-infrared and Raman study of its solid phases. The spectra indicate the existence of a solid-solid transition and we present differential scanning calorimetric (DSC) results as well as X-ray powder diffraction data in evidence of this structural transition. X-ray studies carried out recently[21] show that the point group symmetry of the stable room temperature phase is C_{2h}. On this basis the factor group analysis of the external modes observed in this phase is considered. In the region of the internal modes, vibrational assignments are suggested for many of the spectral lines. Finally, we discuss the possible relevance of the observed solid-solid transition to the occurrence of the mesophase itself.

3.2 Experimental

The transition temperatures were determined using a

hot stage microscope to within ±0.2°C and they are as follows: solid-smectic A (73°C), smectic A-nematic (82.5°C) and nematic-isotropic (106.9°C). Further recrystallization did not significantly improve the nematic-isotropic transition temperature.

The far-infrared spectra were obtained using the Polytec BTR 30 interferometer. The spectral range in this study was 30-240 cm^{-1} and it was covered using spectral range Nos. 2 and 3. Spectra in the two ranges were obtained with resolutions of 3 cm^{-1} and 2.5 cm^{-1} respectively. The polycrystalline samples, about 50 μ in thickness, were contained between two wedged quartz windows. Samples were prepared either with the sieved powder of solvent crystallized material or by slowly cooling down a bubble free film of the isotropic liquid.

Raman spectra were obtained using a Spex 1401 double monochromator in conjunction with a cooled photomultiplier tube and photon counting electronics. The spectra were excited by a He–Cd laser with ~ 10 mw of output power at 4416 Å. Samples were contained in glass capillary tubes and the right angle scattering geometry was used. Finely powdered CBOOA crystallized from n-heptane as well as that solidified from the mesophase were used as samples. Even after about 3 hours of irradiation by the laser beam, the spectra showed no observable changes due to any possible

photodecomposition of the samples. The spectral resolution was ~ 5 cm^{-1}.

DSC experiments were carried out using a Perkin-Elmer differential scanning calorimeter (Model DSC-1B). Samples crystallized from both methanol and n-heptane were used. A heating rate of 4°C/min. was employed and the data were obtained during heating. Both before and after a measurement, the transition temperatures of the sample were checked using the hot stage microscope. No differences were seen and thus it was ensured that there was no contamination of the sample due to the sample pan when the sample was thermally cycled between room temperature and the nematic-isotropic transition point.

The temperature calibration of the DSC instrument in the vicinity of the observed solid-solid transition was checked in two ways. As the peak corresponding to this transition occurs nearly 4° below that of the solid-smectic transition, the known value of the latter transition temperature served as a first check. In addition, the melting temperature of high purity azobenzene (tram), with a known melting point of 68.5°C, was also determined by DSO. In both eases, it was found that the correction to the DSC temperature readings in this region was +4.5±0.2°C.

X-ray powder diffraction photographs were taken using CuK_α radiation and a standard Philips camera of radius

57.3 mm. Typically, exposures of about 10 hours *were* employed.

3.3 Experimental Results and Discussion

(a) Bar-infrared Spectra: We first discuss the far-infrared spectra of polycrystalline CBOOA at room temperature. Trace A of Pig. 3.2 shows the spectrum of sieved powder obtained from solvent-crystallized CBOOA. The spectrum was the same irrespective of whether n-heptane or methanol was used for crystallization. 2he spectrum in this case is characterized by distinct and strong absorption features down to the very low frequency region. Trace B shows the spectrum obtained when the sample was slowly cooled from the mesophase and allowed to solidify, Comparison of the two traces shows that the spectra are markedly different, especially in the region below 180 cm^{-1}. This region would include the external modes, translatory and rotatory, that would be characteristic of a complex molecular crystal. It is seen that the distinct lines present in trace A at frequencies below 120 cm^{-1} are either very weak or almost absent in trace B. In contrast, the strong lines at 128 cm^{-1} and 166 cm^{-1} present in trace B ere not noticeable in trace A. Many similar differences are observed between the two spectra, in the ease of weaker lines as well.

These differences suggest the possible existence of two different polymorphic farms of crystalline CBOOA. Indeed,

FIGURE 3.2

Far-infrared absorption spectra of polycrystalline CBOOA; T = 25°C.

(A) Sample prepared from sieved powder of solvent crystallized CBOOA. She ordinate marks corresponding *to* this trace *are* indicated above the scale break on the right vertical axis.

(B) Sample prepared by solidifying from the mesophase.

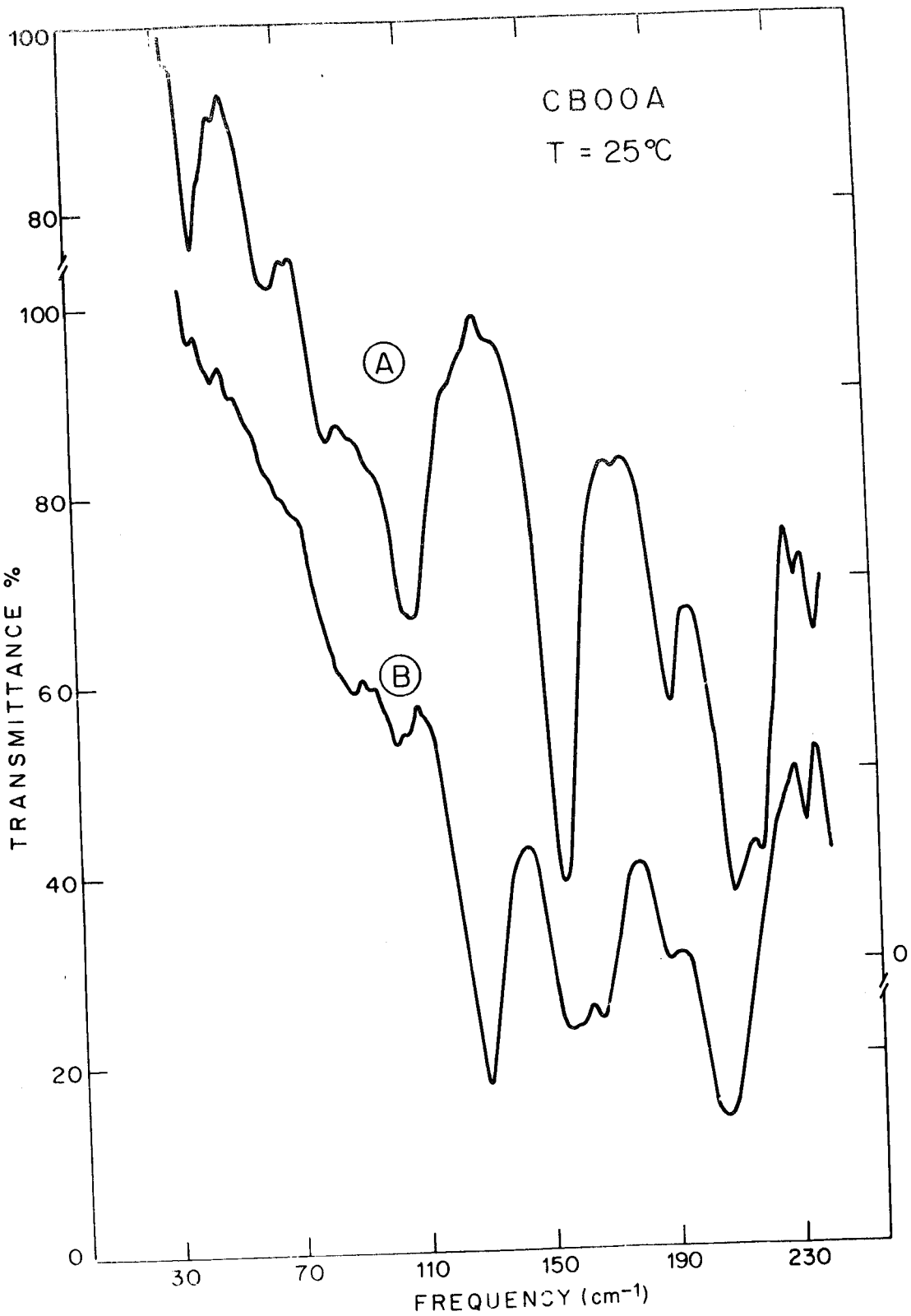
CB00A
T = 25°C
A
B
100
80
100
80
60
40
20
0
0
TRANSMITTANCE %
30
70
110
150
190
230
FREQUENCY (cm⁻¹)

the DSC and X-ray powder diffraction results presented below provide direct confirmation of such a structural change. In the following discussion, the *two* different forms of CBOOA obtained by solvent crystallization and solidification from the mesophase, will be referred to as Phase II and Phase I respectively.

Figure 3.3 shows the temperature dependence of the spectrum of Phase II. It is seen that at 65°C, the spectrum changes abruptly and resembles a temperature broadened version of trace B in Fig. 3.2. In other words, the far-infrared spectra reveal that Phase II transforms to Phase I at 65°C. However, it was noticed. that Phase I can be supercooled to room temperature and remain as a metastable phase for days together. This suggests that the energy barrier separating the two phases is high enough Lo hinder ready and spontaneous conversion to Phase II. Nevertheless, it was established from the spectra that when supercooled, Phase I does convert to Phase II over a period of several hours, if traces of the latter phase were present in the sample. This shows that Phase II fa the thermodynamically stable form of CBOOA below 65°C, while Phase I is the stable form above 65°C ti91 the transition to the smectic phase. While grinding the samples at room temperature, it was also noticed that Phase If could convert to Phase I or vice versa depending upon the energy imparted to the sample during grinding.[21] In the present investigation,

FIGURE 3.3

Temperature dependence of the absorption spectrum of CBOOA initially in Phase II. The sudden change in the spectral features at 65°C arises because of the transition to Phase I.

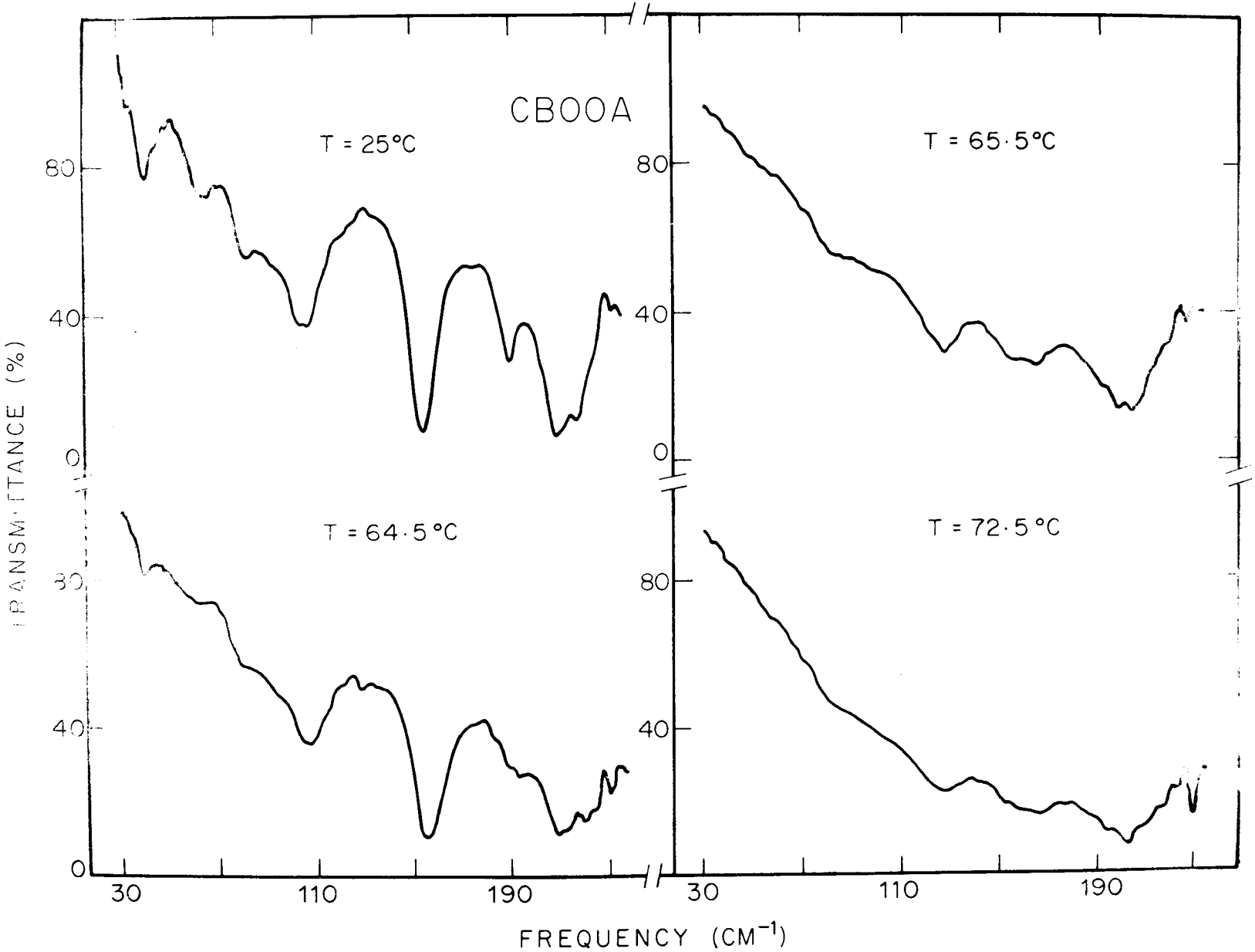
CBOOA
T = 25°C
T = 65·5°C
T = 64·5°C
T = 72·5°C
80
40
0
30
110
190
TRANSMITTANCE (%)
FREQUENCY (CM⁻¹)

these factors were kept in mind and appropriate precautions were taken while obtaining the spectral, thermodynamic and X-ray powder diffraction data on the two phases.

(b) Raman Spectra: Figure 3.4 shows the Raman spectra of polycrystalline CBOOA at room temperature. Traces A and B correspond, respectively, to Phases II and I. In the case of Phase IS, the sample was crystallized from n-heptane and then carefully powdered. The same sample was then melted and solidified for obtaining the spectrum of Phase I. On comparing the two spectra, we again note that marked differences occur below about 200 cm^{-1} and that in this region, the distinct low frequency modes present in Phase II are not noticeable in Phase I. At higher frequencies, however, the two spectra are nearly identical with regard to the observed modes. This is consistent with the expectation that when the crystal symmetry of a complex molecular crystal changes duo Lo a polymorphic transition, the intermolecular modes would be affected to a much greater extent than the intramolecular modes. Indeed, the far-infrared spectra of the two phases of CBOOA also support this expectation.

The use of polycrystalline samples for Raman studies leads to a large amount of stray bight, thereby precluding the observation of very low frequency modes. Hence, we attempted to grow single crystals of CBOOA from a solution

FIGURE 3.4

Raman spectra of polycrystalline CBOOA; T = 25°C. The spectral feature denoted by an asterisk is likely to be due to a plasma line from the laser.

(A) Sample crystallized from n-heptane.

(B) Sample solidified from the mesophase.

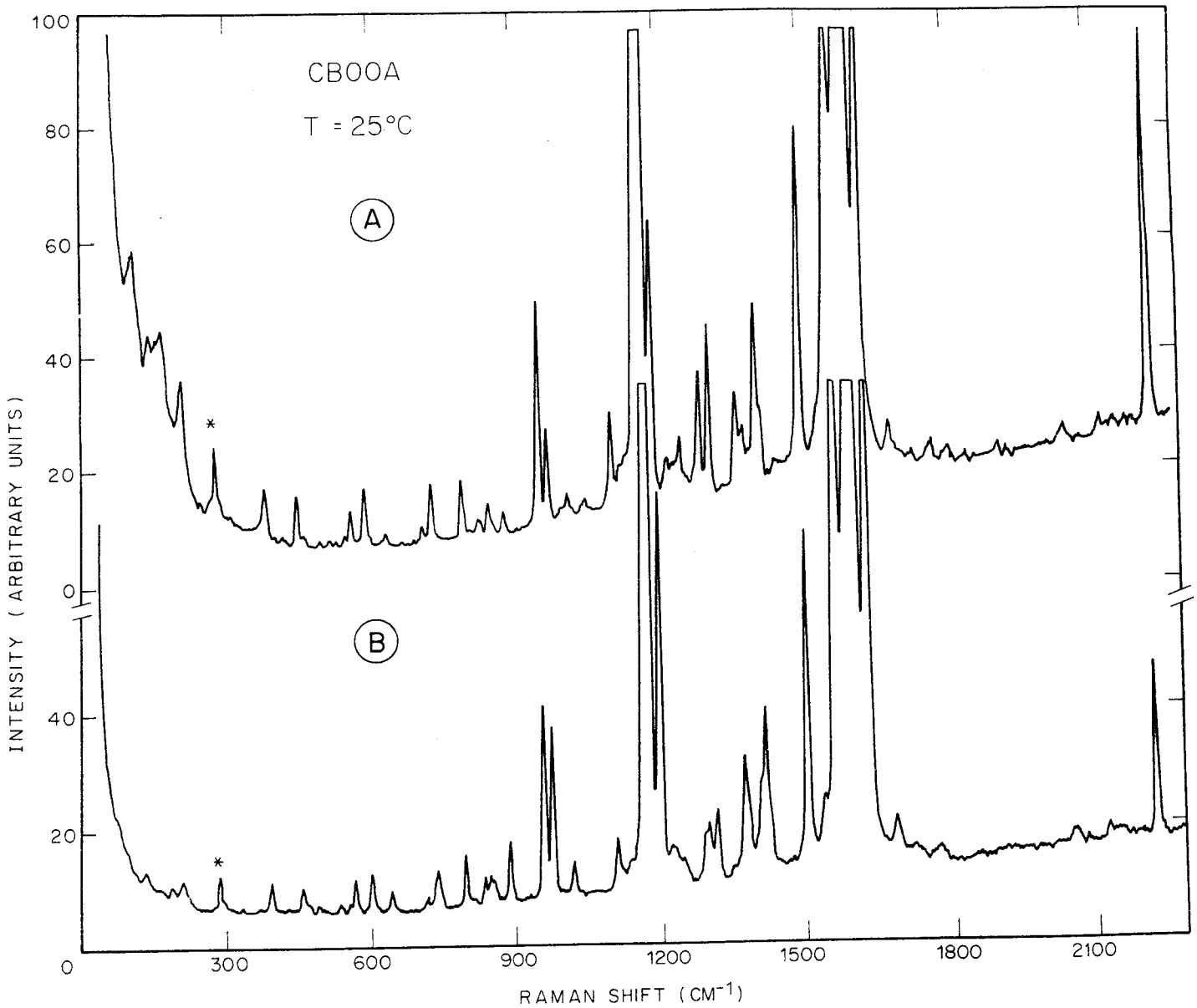
CB00A
T = 25°C
A
B
INTENSITY (ARBITRARY UNITS)
RAMAN SHIFT (CM⁻¹)
100
80
60
40
20
0
40
20
0
300
600
900
1200
1500
1800
2100
*
*

in n-heptane and obtained thin platelets with the typical dimensions *0.5* x 1.5 x 2 mm. However, the crystals contained many flaws and hence cutting, polishing and orienting them proved difficult. Consequently, we have used an unoriented single crystallite in Phase II and obtained its Raman spectrum in the 30-150 cm^{-1} range. Trace A of Fig.3.5 shows that additional low frequency modes are observed in this case as compared to Fig 3.4. In order to obtain a corresponding spectrum of a single crystal of Phase I, the crystal was first heated to 66°C. However, it became opaque and polycrystalline in this process. This could arise from strains in the crystal *or* a disruptive volume change attending the transformation to Phase I. Nevertheless, the sample, now in Phase I, yielded a low frequency spectrum in the same range under a comparable stray light level and this is shown in trace B. It is clear that again the low frequency modes axe extremely weak in Phase I.

It is of interest to consider the vibrational spectra of the two phases, in relation to the crystal symmetry of both phases. Detailed structural data are available at this time only for Phase II. X-ray studies on single crystals grown from n-heptane indicate[20] that the crystal structure of Phase II belongs to the space group $C_{2h}^5(P2_1/a)$. The primitive unit cell possesses the point group symmetry C_{2h} with four molecules of CBOOA situated at sites having

FIGURE 3.5

Low frequency Raman spectra of crystalline CBOOA at 25°C.

(A) The sample in this case is a single crystal grown from a solution of CBOOA in n-heptane.

(B) Spectrum obtained when the sample corresponding to trace A was heated to 66°C and then cooled to room temperature. The resultant sample, however, was not a single crystal.

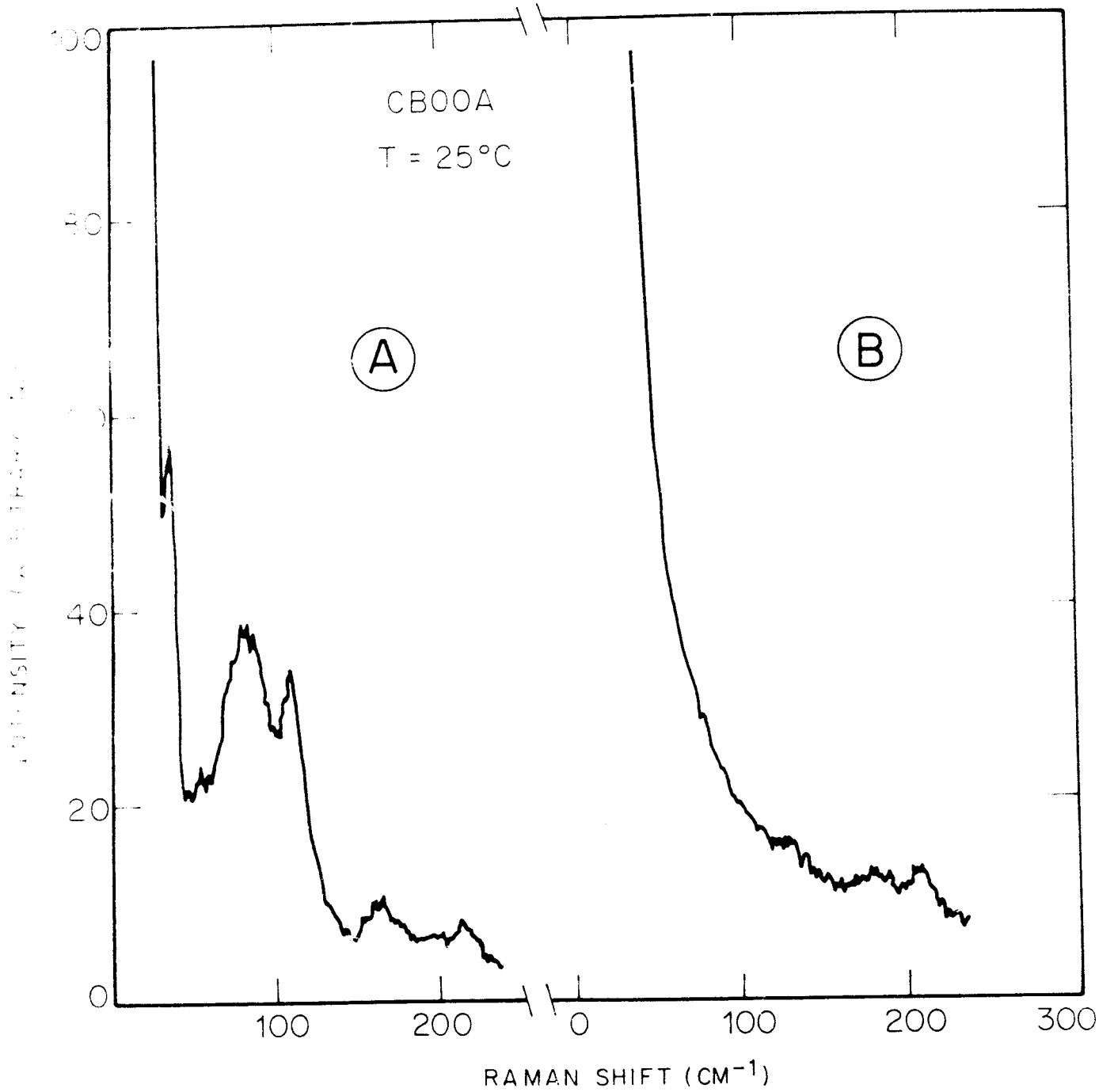
CB00A
T = 25°C
A
B
0
20
40
100
200
0
100
200
300
RAMAN SHIFT (CM⁻¹)

C_1 symmetry. The coupling between the four molecules in the unit cell would lead to 24 zone-center external or lattice modes. As shown in Appendix A, a factor group analysis using the method of coupling[22] shows that all of them are non-degenerate modes and their representation is given by $6A + 6B_g + 6A_u + 6B_u$. Among these, We three acoustic modes belong to $A_u + 2B_u$ and the representation of tho external optical modes is given by $6A_g + 6B_g + 5A_u + 4B_u$. Modes of A_u and B_u symmetry are infrared active and Raman inactive while *those* of A_g and B_g symmetry are Raman active and infrared inactive. However, accidental degeneracies may occur between the Raman and infrared active modes. If suitable single crystals become available, it would be of interest to carry out polarization studies and determine the symmetries of the observed low frequency modes in both phases.

As noted earlier, the Raman spectra of the two phases show no marked differences in the internal mode region. In this region, the vibrations of the CBOOA molecule would include those modes which are characteristic of the distinct molecular units comprising CBOOA. The free CBOOA molecule possesses the point group symmetry C_1 and hence all of its internal modes would be infrared as well as Raman active. In the crystalline state, tho coupling between the different CBOOA molecules in the unit cell can, in principle, cause each of these internal modes to split further into infrared

and Raman active modes. Considering the frequencies of the vibrational modes observed in this study, we have made an attempt to correlate many of them with the characteristic vibrations of the different molecular units constituting CBOOA.

Tables 3.1 and 3.2 list, respectively, the observed far-infrared and Raman frequencies in both phases of solid CBOOA. Possible correlations with characteristic group vibrations of the CBOOA molecule are also suggested in several cases. As indicated in the tables, there is some overlap between the frequency regions of the various possible modes. In addition, designations such as rocking and twisting modes are only approximate as considerable coupling between these motions can occur In a complex molecule. For these reasons, complications can arise in the assignments of some of the modes. Nevertheless, when the present spectra are compared with those of other liquid crystalline materials[1,3,23] as well as organic compounds that contain structural groups similar to those comprising CBOOA, a tentative correlation of several of the observed modes with characteristic group vibrations can be made. The present assignments have been proposed on this basis.

(c) Differential Scanning Calorimetry: As discussed earlier, the thermal characteristics of the two phases as well as *the* metastable nature of Phase I below 65°C, could

be inferred from the far-infrared spectra. DSC measurements were undertaken in order to obtain direct evidence of the solid-solid transition and also determine the latent heat of this transition.

Figure 3.6 shows the typical DSC results. In trace 1, the sample used was recrystallized from n-heptane. We note that there is a distinct endothermic peak at 68.8°C in addition to fhe peak at 73°C. The latter peak represents the solid-smectic transition and is shown truncated in all the four traces. The peak centered at 68.8°C provides direct evidence of a transformation occurring in the solid phase. To within 10%, the corresponding energy of transition is estimated to be 2030 cal/mole. Trace 2 shows the DSC curve obtained after resolidifying the sample and cooling it to room temperature. The peak at 68.8°C is absent now and this confirms that when solidified from the mesophase one obtains Phase I, which becomes supercooled and exists below the transition temperature as a metastable form. Traces 3 and 4 are, respectively, the analogues of traces 1 and 2 except that the starting sample had been crystallized from methanol. We note that the solid-solid transition peak is distorted on the low temperature side due to the presence of additional structure. We feel that one of the possible contributing factors could be the presence of methanol in the crystal as solvent of crystallization. Then, upon heating, it would disappear from the crystal

FIGURE 3.6

Differential scanning calorimetric (DSC) data of CBOOA in the vicinity of the solid-smectic transition.

1) Sample crystallized from n-heptane.
2) DSC curve obtained when the sample corresponding to trace 1 was taken to the isotropic phase, then solidified and cooled down to room temperature.
3) Sample crystallized from methanol.
4) DSC curve obtained when the sample corresponding to trace 3 was taken to the isotropic phase, then solidified and cooled down to room temperature.

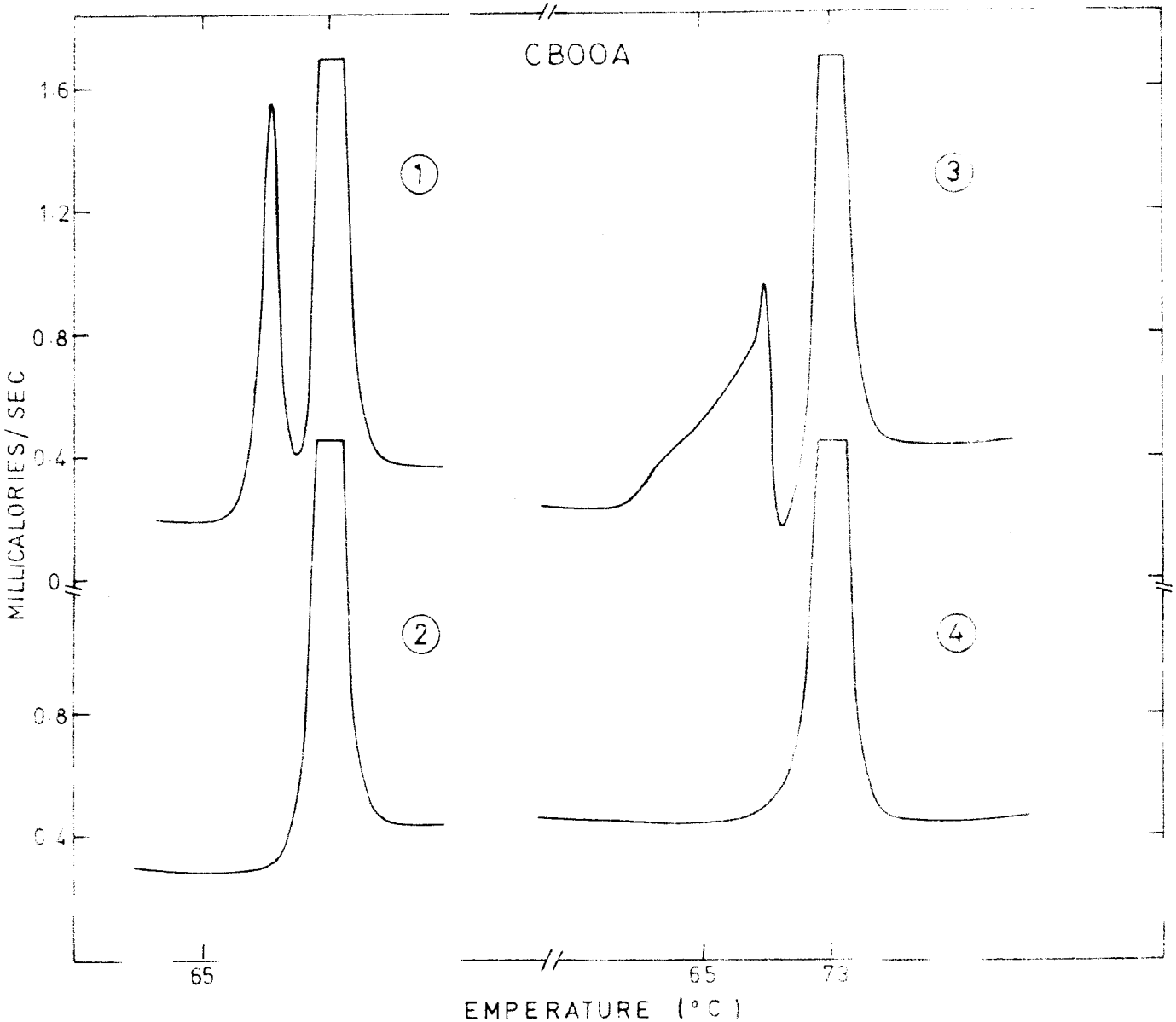
CBOOA
1.6
1.2
0.8
0.4
0
0.8
0.4
MILLICALORIES / SEC
1
2
3
4
65
65
73
EMPERATURE (°C)

at ~ 65°C, giving rise to the additional structure. This point could be checked further by cooling the sample below the freezing point of methanol and observing the peak corresponding to the 'melting' of methanol at - 94°C. We were unable to perform this check as the DSC instrument was limited by its temperature range.

The solid-solid transition temperature as determined from the peak In trace 1 is 68.8°C. However, as seen from Fig.3.3, the far-infared spectra indicate that the transition sets in at ~ 65°C. This apparent discrepancy is reconciled by noting that in trace 1 of Fig.3.6, the onset of the transition occurs at ~ 65°C and the peak merely denotes the temperature at which energy is being absorbed at the maximum pace. Thus, if a sample in Phase II is maintained at ~ 65°C for a sufficient length of time, as was the case during far-infrared measurements, it would absorb energy and change over to Phase I.

It is of interest to note here that Cladis[19] and Hardouin et al.[16], respectively, have earlier reported differential thermal analysis as well as specific heat measurements on CBOOA. However, no evidence for the solid-solid transition was reported in either study. Presumably, this is because in both cases the starting sample may have been solidified from the mesophase and thus existed in Phase I to begin with.

(d) X-ray Diffraction Data: X-ray powder photographs of both phases were obtained at room temperature. As Phase I is metastable at room temperature and grinding may cause interconversion between the two phases, it is necessary to unambiguously ascertain the phase of the sample, in order to avoid discrepancies or apparent anomalies in the X-ray data. Hence, we observed the following precautions. In the case of Phase XI, the sample crystallized from n-heptane was carefully powdered imparting minima3 force. Then it was allowed to stand for about 30 hours to facilitate complete conversion to Phase II, before the X-ray exposure was commenced. The phase of the sample was also confirmed by its far-infrared spectrum in the region below 150 cm^{-1}. In the case of Phase I, the exposure was commenced immediately after careful grinding. Simultaneously, using a portion of the sample, the far-infrared spectrum was recorded at different time intervals. It was thus ensured that for the duration of the X-ray exposure, the sample indeed did remain in Phase I without undergoing any appreciable conversion to Phase II.

Figure 3.7 shows the respective densitometer traces of the powder photographs of the two phases. In the case of Phase i, the powder photograph revealed streaks of additional darkening near the equatorial plane, for the three diffraction maxima lying within the angular range

FIGURE 3.7

Densitometer traces of X-ray powder diffraction photographs of CBOOA in the two phases; T = 25°C. (A) and (B) here have the same connotation as in the caption of Figure 5.4

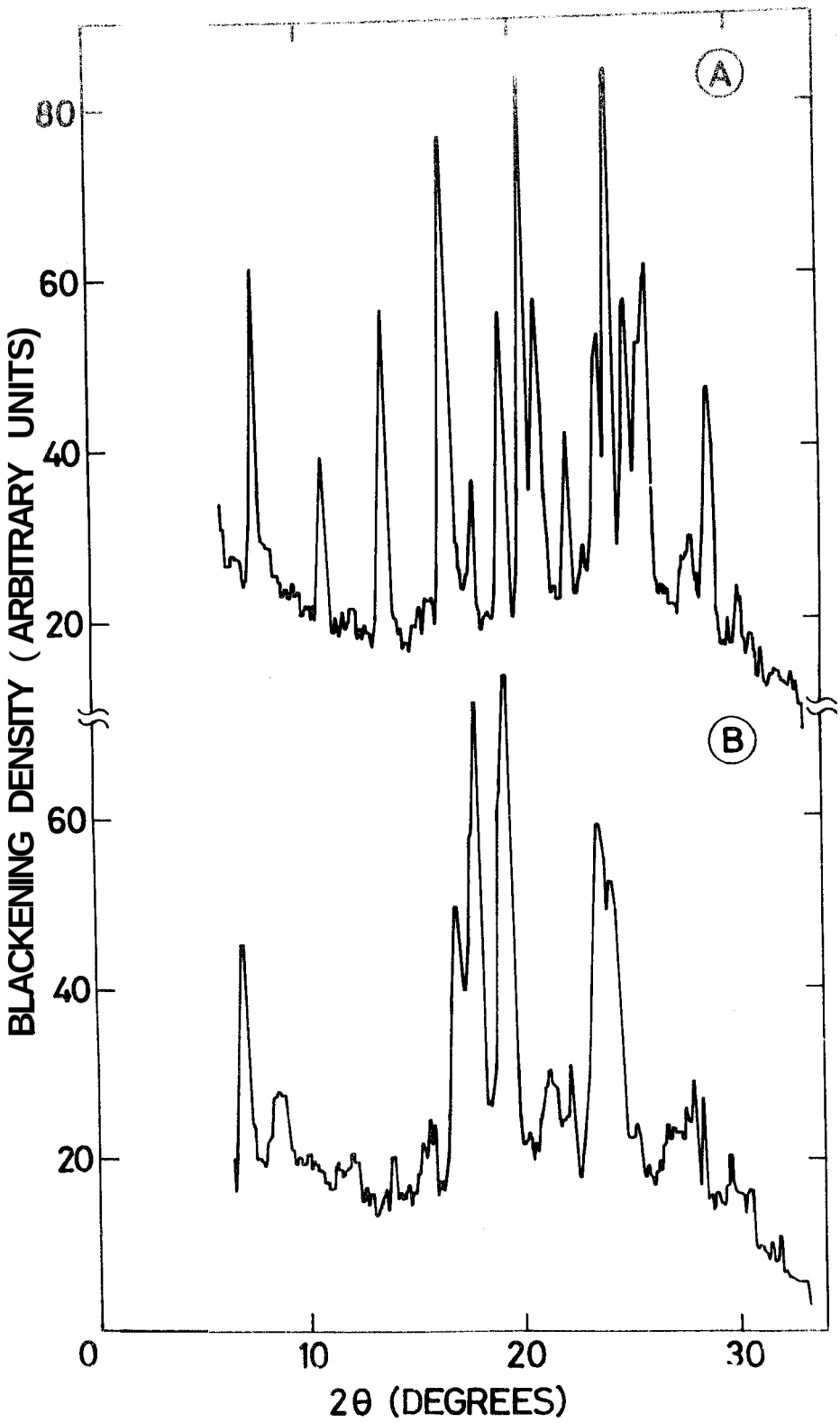
A
B
80
60
40
20
60
40
20
0
10
20
30
BLACKENING DENSITY (ARBITRARY UNITS)
2θ (DEGREES)

16-20°. Hence ths densitometer trace also shows a corresponding enhancement in the peak intensities of these three diffraction maxima. It is not clear at this time whether the additional streaks of darkening represent a genuine effect or they arise due to some artifact of the experimental conditions. Nevertheless, it can be seen that the two traces in Pig. 3.7 exhibit marked differences with regard to the diffraction maxima observed in each case. This shows that the two phases clearly differ in their crystal structure.

3.4. Conclusions

From a study of the vibrational spectra of CBOOA we have demonstrated that it possesses two distinct solid phases. In particular, we note that it was possible to elucidate their stability regions as well as their thermal behaviour through the study of their far-infrared spectra alone. Both the DSC and the X-ray results indicate that the two phases differ markedly in their struoture and molecular packing and this fact is also evident from their low frequency infrared and Raman spectra.

Previous studies on mesogens have shown that monotropic solid phases can be? obtained in some cases by cooling the liquid crystaline phase, The low frequency vibrational spectra of the monotropic solid phases have been studied in the cases of p-azoxyanisole[5] (PAA) and p-methoxybenzylidene-

p'-n-butylaniline[23] (MBBA). In both these cases, the spectra of the monotropic phases show certain differences when compared to their respective stable phases, especially at frequencies below 150 cm^{-1}. This behaviour is in general agrement with that reported hers for the two phases of CBOOA. The spectral changes indicate that in all these oases the molecular ordering within the crystal is different between the stable and metastable phases. In spite of this broad similarity, the observed thermodynamic behaviour of CBOOA is distinctly different from that seen in the cases of PAA[24] or MBBA.[25] In the latter two *oases, either* the stable phase ox the metastable monotropic phases can fuse and directly transform to the mesophase. However, this is not the oase in CBOOA. In this case, even if one starts with the stable solid, Phase II, the formation *of* the mesophase always proceeds via the transition to Phase X. In other words, Phase II becomes thermodynamically unstable prior to the occurrence of the smectic A phase. Furthermore, as Phase I can also be formed while approaching the smectic A phase from below, it cannot be regarded as a monotropic form.

It thus appears reasonable to regard the transition from Phase IS to Phase I as a pre-transition effect. Pre-transition phenomena exhibited by the solid phases of mesogens and their relevance to the formation and structure *of* the mesophase itself have evoked *recent* interest. For

example, Wendorff at al.[26] have carried out an X-ray study of cholesteryl esters and find that slightly below their melting point, the order in directions normal to the long axes of the molecules decreases markedly. They interpret this as an anticipation of the transition to the mesophase which, of course, exhibits complete disorder in directions normal to the long axes of the molecules. Also, from an infrared study of p-azoxyanisole and its higher homologues, Bulkin at al.[7] noted that as the crystal-nematic transition is approached, several infrared bands disappear gradually. They attribute this phenomenon to the creation of lattice defects due to the movement of the molecules from lattice to interstitial sites. The existence of a 'soft solid' region below tho crystal-nematic transition has also been suggested in the cases of p-azoxyanisole[27,28] and p-methoxybenzylidene p'-n-butylaniline.[23]

The transition in CBOOA from Phase II to Phase I occurs just below the onset of the smectic A phase. It is thus of interest to consider whether this solid-solid transition represents an anticipation of the transition to the smectic A phase. If so, the structure of Phase I would reflect a corresponding lowering of crystalline order. From the infrared and Raman spectra, we note that certain low frequency nodes are considerably broadened or attenuated in Phase I as compared to Phase II. This

would imply that the corresponding degrees of freedom associated with the molecules are well coupled in Phase II, whereas in Phase I they tend to become more uncorrelated and diffusive, thereby reducing the crystalline order as well, The additional degrees of freedom thus activated may relate to the entire molecule or they could be intramolecular in character. The latter case is of importance considering the presence of the relatively flexible octyloxy tail in the CBOOA molecule and the role played by conformational changes in the alkyl chains near many phase transitions.[6,29] As suggested by Andrews,[30] the latent heat associated with the transition from Phase II to Phase I can arise, in part, if one assumes the onset of a 'melting' disorder of the octyloxy tail. However, any calculation of the latest heat of the transition on this basis must take account of the fact that the newly accessible conformations of the actyloxy tail would be limited by the coupling of the tail with the phenyl ring. In addition, further disorder associated with the orientation of the CH=N grouper and the phenyl rings may also exist. 31 These considerations as well as the low frequency spectra reported here suggest that the structure of Phase I can be expected to be more disordered than that of Phase II. The large endothermic peak observed in the DSC trace at the Phase II-Phase I transition also supports this idea. Further crystal structural and neutron scattering data on both phases should prove useful in elucidating the nature

sf the solid-solid transition and in ascertaining whether St is indicative of a pre-transition that anticipates the formation of the mesophase.

References

1. W. Maier and G. Englert, Z. Physik Chem. (NF) 19, 168 (1959).

2. N.M. Amer, Y.R. Shen and H. Rosen, Phys.Rev.Lett. 24, 718 (1970).

3. N.M. Amer and Y.R. Shen, J. Chem. Phys. 56, 2654 (1972).

4. A.S. L'vova, L.M. Sabirov, I.M. Arefev and M.M. Sushchinskii, Opt. Spectrosc. 24, 322 (1968).

5. J.M. Schnur, M. Hass and W.L. Adiar, Phys.Lett. 41A, 326 (1972).

6. J.M. Schnur, Mol.Cryst. and Liq. Cryst. 23, 155 (1973).

7. B.J. Bulkin, D. Grunbaum and A.V. Santoro, J.Chem.Phys. 51, 1602 (1969).

8. B.J. Bulkin and WB Lok, J.Phys.Chem. 77, 326 (1973).

9. S. Venugopalan, Pramana, Suppl. 1, p. 167 (1973).

10. N.M. Amer and Y.R. Shen, Solid State Commun. 12, 253 (1973).

11. J.M. Schnur and M. Fontana, J. de Physique 35, L53 (1974).

12. P.G. de Gennes, C.B. Acad. Sci. (Paris) B274, 758 (1972).

13. P.G. de Gennes, Solid State Commun. 10, 753 (1972).

14. W. McMillan, Phys. Rev. A4, 1238 (1971); A8, 1921 (1973).

15. K.K. Kobayashi, Mol. Cryst. Liq. Cryst. 13, 137 (1971); Phys. Lett. 31A, 125 (1970).

16. F. Hardouin, H. Gasparoux and P. Delhaes, J. de Phys. 36, Suppl., C-1:127 (1975).

17. G. Wand, Pramana, Suppl.1, P23 (1973)

18. N.V. Madhusudana, P.P. Karat and S. Chandrasekhar, Pramana Suppl. 1, p. 225 (1973).

19. P.E. Cladis, Phys. Rev. Lett. , 1200 (1973).

20. G.V. Vani and K. Vijayan, Mol.Cryst.Liquid Cryst. 42, 249 (1977).

21. A.W. Baker, J. Phys. Chem. 61, 450 (1957).

22. L. Couture and J.P. Mathieu, J.Phys.Radium 10, 145 (1949).

23. E. Sciesinska, J. Sciesinski, J. Twardowski and J.A. Janik, Mol.Cryst.Liquid Cryst. 27, 125 (1974).

24. R.C. Robinder and J.C. Poirier, J.Am.Chem.Soc. 90, 4760 (1968).

25, J. Mayer, . Waluga and J.A. Janik, Phys.Lett. 41A, 102 (1972).

26. J.H. Wendorff and F.P. Price, Mol.Cryst.Liquid Cryst. 22, 85 (1973).

27. R. Pynn, K. Otnes and T.Riste, Solid State Commun. a, 1365 (1972).

28. T. Riste and R. Pynn, Solid State Commun. 12, 409 (1973).

29. A.R.Ubbelohde, Melting and Crystal Structure (Oxford University Press, 1965).

30 J.T.S. Andrews, Phys. Lett. 46A, 377 (1974).

31. J.A. Janik, J.M. Janik, J. Mayer, E. Sciesinska, J. Sciesinski, J. Twardowski, T. Waluga and W. Witko, J. de Phys. 36, Suppl.3, C1-159 (1975).

Table 3.1. Far-infrared absorption frequencies f in cm^{-1}) of the two phases of CBOOA at 25°C, in the range 30-220 cm^{-1} and their proposed assignments*. The frequencies are accurate to ± 1 cm^{-1}.

Phase II	Phase I	Proposed assignment
33 (sh)		
40	45 (vw)	
49 (sh)		$\tau(CH_2CH_2)$
64	70 (sh)	
82	84 (sh)	∠C-C-C bend (C_8H_{17})
	88	
94 (sh)	93 (sh)	Libration C_6H_4
	98	
	101	
107		
122 (sh)	128	$\tau(CH_2CH_2)$
136 (sh)		
154	157	
	166	
190	187	
208	204	$\tau(CH_3)$
217	219 (sh)	

Lattice modes

*Note: sh = shoulder, vw = very weak.
The symbols describing the proposed assignments are given in Table 3.3.

Table 3.2. Raman shifts (in cm^{-1}) of the two phases of CBOOA at 25°C, in the range 30-2300 cm^{-1} and their proposed assignments. The Raman shifts are accurate to ± 3 cm^{-1}.

Phase II	Phase I	Proposed assignment	
34			Lattice modes
70 (sh)	64 (sh)	$\tau(CH_2CH_2)$	
80	86 (sh)	Libration C_6H_4	
106	96 (sh)		
	124 (sh)		
138	130	$\tau(CH_2CH_2)$	
160	175	$\tau(CH_2)$	
165	182 (vw)		
203			
212	205		
378	360 (vw)	Libration CHN	
	389		
	422 (vw)		
445	454		C_6H_4-C=N interaction
490 (vw)	486 (vw)	∠C-C-C bend (C_8H_{17})	
512 (vw)			
527 (vw)	532 (vw)		
543 (vw)	552 (vw)		
555	562		
585	596		
628	636		
703	713 (vw)		

Phase II	Phase I	Proposed assignment			
724	734	$\rho(CH_2)$			
788	792	ω			
806 (vw)					
824	830 (vw)	γ	$\rho(CH_2)$		
842	842 (vw)				
	852 (sh)				
873	883	$\rho(CH_3)$			
948	955	γ			
965	972				
1007 (vw)	1015	δ		ω_c	
1043 (vw)					
1100	1106				
1131 (sh)	1133 (vw)	$\tau(CH_2)$	δ		
1163	1166	ω_c			
1189	1195				
1220 (vw)	1219 (vw)	$\gamma(CH_2)$			
1234 (vw)					
1249	1243 (vw)	C-O-C stretch			
1287	1286		ω		
1307	1294			$\tau(CH_2)$	
	1310				$\gamma(CH_2)$
	1344 (sh)				
1364	1370	$\delta(CH_3)$			
1376 (vw)					
1402	1404 (sh)				
1412 (sh)	1411				

Phase II	Phase I	Proposed assignment
	1418	
1444 (vw)		$\delta(CH_2)$
1495	1498	ω ; $\delta(CH_3)$
1532 (sh)	1536	
1557	1560	
1587	1591	ω ; C=N stretch
1621	1622	
1678	1680	
1724 (vw)	1718 (vw)	γ overtones?
1767 (vw)	1769 (vw)	
1800 (vw)		
2046 (vw)	2050 (vw)	
2115 (vw)	2122 (vw)	
2225	2218	C≡N stretch

*Note: The note under Table 3.1 is applicable here also.

Table 3.3

Notation used in describing the vibrations (from Ref. 1)

Vibration		Symbol
Phenyl group vibrations		
C-C- and C-C-X vibrations		
in-plane vibrations	—	ω
out-of-plane vibrations	—	Γ
C-H deformation vibrations		
in-plane vibrations	—	δ
out-of-plane vibrations	—	γ
Alkoxy group vibrations		
chain ofbrations		
$-O-CH_3$	—	ω_{C-O}
-O-C-C-	—	ω_C
chain twisting	—	$\tau(CH_2CH_2)$
CH_2 vibrations		
scissoring deformation	—	$\delta(CH_2)$
CH_2 wagging	—	$\gamma(CH_2)$
CH_2 twisting	—	$\tau(CH_2)$
CH_2 rocking	—	$\rho(CH_2)$
CH_3 vibrations		
symmetric- and assymmetric-deformation	—	$\delta(CH_3)$
CH_3 wagging (in C-C- plane)	—	$\gamma(CH_3)$
CH_3 twisting	—	$\tau(CH_3)$
CH_3 rocking (perpendicular to C-C- plane)	—	$\rho(CH_3)$